Numerical Study of The Power Plant Surface Condenser to Prevent High Pressure in Critical Areas

Eky Novianarenti[1], Ary Bachtiar Khrisna Putra[2], Setyo Nugroho[3], Arrad Ghani Safitra[4], Rini Indarti[5], Priyambodo Nur Ardi Nugroho[6], Mohammad Basuki Rahmat[7]

[1, 5, 6, 7] Politeknik Perkapalan Negeri Surabaya, Indonesia
[2] Institut Teknologi Sepuluh Nopember Surabaya, Indonesia
[3, 4] Politeknik Elektronika Negeri Surabaya, Indonesia

Corresponding author:
Eky Novianarenti
Politeknik Perkapalan Negeri Surabaya, Indonesia
E-mail: ekynovianarenti@ppns.ac.id

Abstract – Font 11

A numerical study to reduce the condenser pressure in critical areas of a power plant surface condenser has been carried out. Numerically, effects are considered through a three-dimensional simulation approach. Modifying by adding a guide plate with a three variation of angle, (α) 15º, 30º, 45º in the surface condenser area to reduce the dynamic forces and pressure due to the collision of fluid flow in the critical pipeline without reducing the purpose of the design of shell and tube heat exchanger results in transferring heat. The drag force caused by the interaction of the shear layer with the surface of the body is very undesirable, so that the control of the flow fields is needed, one of which is by optimal angle guide plate of the pipe arrangement in the critical area. This study aims to determine the optimal plate angle to overcome high pressure in the critical area. This research was numerically conducted using 3D CFD ANSYS 14.5 software with a turbulence model using a standard k-ε using a pressure-based solution solver. The initial stage takes geometric data on the surface condenser in the design specification as the basis for making the domain and data from before as boundary conditions in the simulation research process. The result is that with the addition of guide plates, the average drag coefficient (Cd) is reduced compared to the average Cd in the baseline conditions and angle variation (α) 15º, 30º, 45º is 0.537; 0.644; 0.446; 0.464. Taking into this aspect, the most optimal plate angle is 30º. The simulation results show that changing the angle of the plate can reduce the Nusselt value than the baseline conditions.

Keywords: *power plant surface condenser, angle, guide plate, critical area, pressure.*

INTRODUCTION

The condenser is one of the essential components in an energy generation system based on steam. The most significant energy loss occurs in the condenser in the power generation cycle due to a large amount of steam from the exhaust turbine condensed back into the liquid phase. The condenser becomes a vacuum due to changing the vapor phase to the liquid phase in it. The higher the vacuum in the condenser, the turbine efficiency will increase. The greater is the vacuum that occurs in the condenser, the lower the pressure of the turbine, and efficiency will increase. Low pressure on the exhaust turbine lower the steam saturation temperature, and the saturation temperature lower, much energy is wasted before the steam is condensed. When more energy is wasted, the efficiency will increase. Thus the efficiency of the condenser operation needed to maintain turbine efficiency stays high [1].

Based on data from the performance test at a steam power plant, it shows that there is a decrease in performance on the surface condenser equipment, which is a shell and tube heat exchanger in the form of a decrease in heat transfer value, and there is a reasonably high noise condition on the surface condenser. The turbulent flow conditions may be relatively high, resulting in high-pressure drop values and quite high vibrations in the tube surface condenser arrangement. The decrease in performance can affect the overall efficiency of the power plant. Haldkar V [2] states that the decrease in surface condenser performance is either caused by the deviation of the cooling water inlet temperature, flow rate deviation, and surface condenser pressure can cause a decrease in power plant efficiency by an average of 2.7%. So it can be said that the surface condenser as a heat absorber has an essential role in creating reliable power plant performance. So it is necessary to carry out proper operation and maintenance, and engineering modifications to the surface condenser to maintain or improve the performance of the surface condenser [3-4].

With the decrease in the performance value of the heat exchanger above, maintenance actions in the form of chemical cleaning are carried out, and several tests such as eddy current test, non-destructive test, vibration measurement, and metallography test. From the maintenance and testing measures, it was found that there was tube damage. Based on the manual book [5-6], it is stated that the heat exchanger uses a titanium tube. So that the decrease in heat exchanger performance due to corrosion problems can be ignored because titanium has a reasonably high resistance to various types and forms of corrosion. So most likely, the problem of damage to the tube heat exchanger is due to the flow of steam that is not well controlled. The discharge and velocity of the steam entering the heat exchanger are large enough to cause vibration in the heat exchanger tube, and within a certain period, it will cause friction between the tubes or the baffles resulting in tube damage. The ones were found in various locations, most of which were located in the tube area that received a high vapor flow load (**critical area**), some occurred in the area near the tube sheet at the outlet of the heat exchanger and around the tube that was closed (plugging tube).

The area marked by the circle in Figure 1 is the area that receives the most significant dynamic force. This area is called the **critical area** where the tube damage occurs the most. The dynamic forces acting on the tube are the drag force in the flow direction and the lift force perpendicular to the flow. The following is a picture of the position of the critical area in the tube heat exchanger arrangement where this area receives a high steam flow load, so that tube damage is found around it. A simple geometric model is made to obtain local data parameters and determine the influence parameters separately to carry out the tube bank's physical flow and heat transfer process. However, several papers discuss the measurement of local parameters of cross-

flow in tube banks. The flow characteristics of the steam condenser depend on supporting data about the tube arrangement under adiabatic conditions and isothermal flow. As it passes through the cylinder, the viscous fluid flow has characteristics such as stagnation, boundary layer, separation, and the wake behind the tube. In comparison, the cylinder submerged in the viscous fluid experiences a drag force and a lift force.
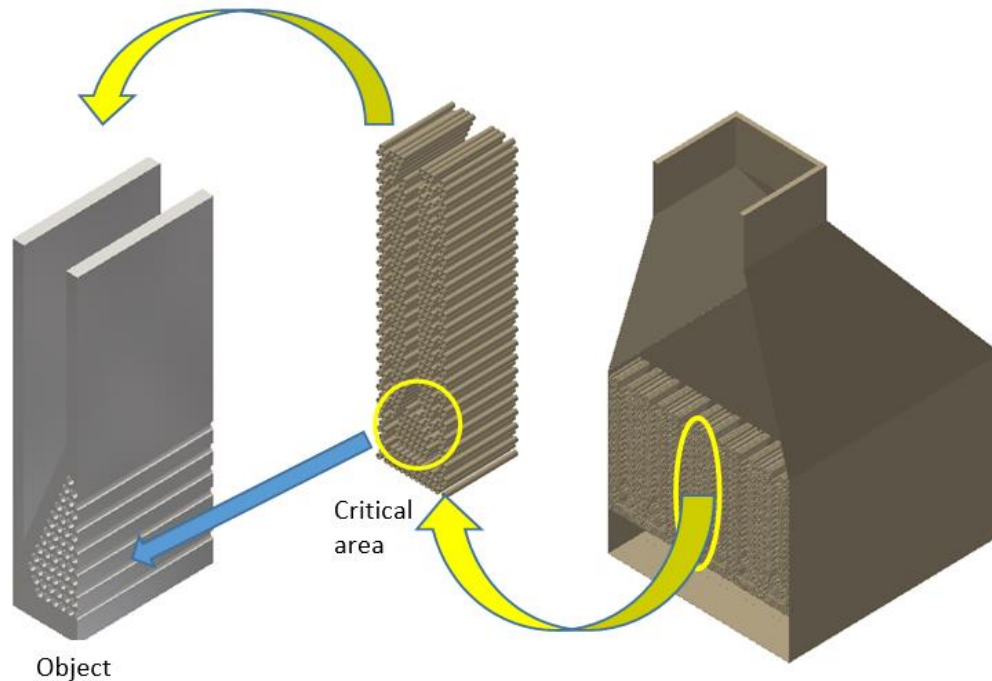

Figure 1. Cross-section of the Condenser

Tensile forces are closely related to flow separation. The earlier the separation occurs, the wider the wake area so that the drag force increases. Therefore, controlling the fluid flow field through a passive method is very useful in reducing the drag force. In terms of heat transfer, the highest heat transfer value in a cylinder is generally located at the stagnation point, reaching the lowest temperature at the separation point. So by delaying the separation point on the cylinder, it increases the heat transfer value in the cylinder. Therefore, many studies have been carried out to reduce the drag force contained in the bluff body.

Furthermore, reducing the drag force and suppressing vortex shedding was carried out by Qiu et al. [7] with a circular cylinder-mounted splitter plate in the wake area. Circular cylinder with a diameter of 0.4 m to distinguish aerodynamically from a bare cylinder roof. The results determine the position of the separation point related to the location and thickness of the boundary layer and determine the size and strength of vortex shedding due to interactions between vortexes related to the magnitude of the pressure in the building and the formation of a large unsteady force where vortex shedding has the potential to damage the tube structure.

A numerical study about tube arrangement in power plant surface condenser is conducted by Chakrabarty S.G et al. [8], Hui Zeng et al. [9] with three typical tube arrangements were considered. The result is that the new arrangement is better than the HEI standard. The other numerical model developed condenser in coal-fired power plants by Vedran et al. [10] uses steady-state conservation laws for mass and energy. Algorithms are described and explained. The validation using the measurement from existing coal-fired power plant condenser.

Another research that has a role in increasing heat transfer in the tube is by adding a device to cause a vortex (vortex generator), among others, by Chu et al. [11] varied the angle of attack (α= 15º, 30º, 45º and 60º) and the number of tube rows (2, 3, 4, and 5) on the oval tube banks fin heat exchanger arranged staggered. The research, carried out by numerical simulation, got the optimal heat transfer performance at configuration α= 15º with tube rows 2. Furthermore, Lotfi et al. [12] have researched thermohydraulic performance numerically on the smooth wavy fin and elliptical tube (SWFET) by varying 4 new VGs, namely rectangular trapezoidal winglet (RTW), rectangular angle winglet (ARW), curved angle rectangular winglet (CARW) and wheeler wishbone (WW). In the VG winglet type geometry, the angle of attack (α= 15º, 30º, 45º, 60º, and 75º). The results show that CARW obtains the best increase in heat transfer at α= 15º and RTW at α= 75º. Therefore, a numerical study was conducted that displays flow visualization in 3D is able to explain in more detail the physical mechanism of flow in the critical area region by developing angle variation.

NUMERICAL METHOD

Turbulent flow is recognized by the presence of a fluctuating velocity field. These velocity fluctuations carry various quantities such as momentum, energy, particle concentration so that these quantities also fluctuate [13]. These fluctuations can occur on a small scale and have a high frequency, so it is too complicated and heavy to be calculated directly in practical engineering calculations, even using sophisticated computers. Therefore, the related equations can be averaged (time-averaged, ensemble-averaged) or manipulated to eliminate small-scale fluctuations. Thus, these equations can be more easily solved. However, there are additional unknown variables in the modified equation, and turbulence models are needed to determine these variables.
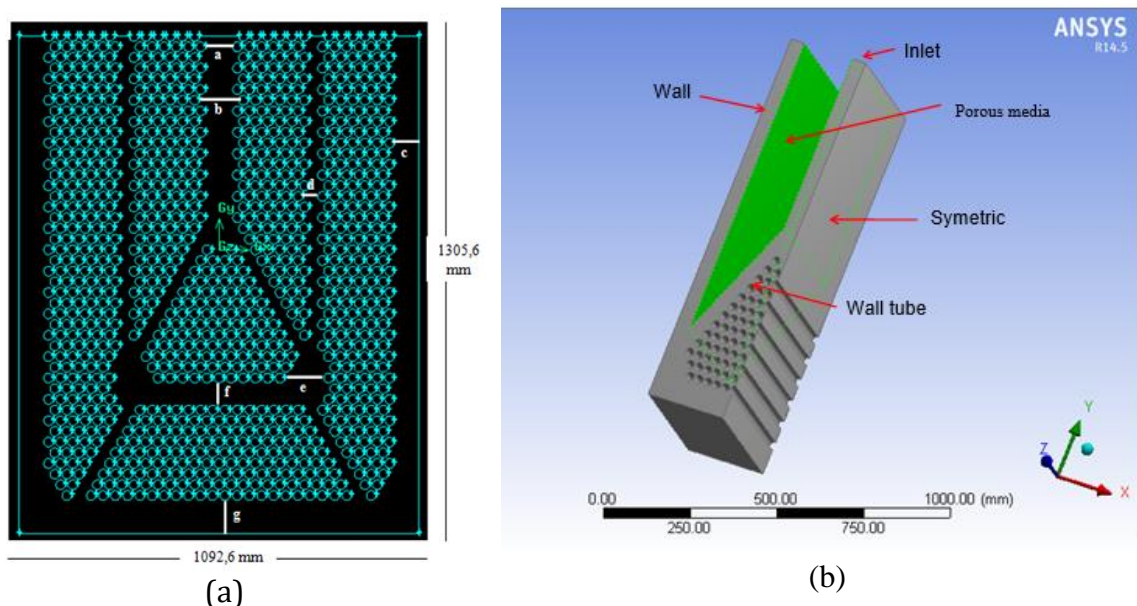

(a)

(b)

Figure 2. Configuration of the condenser (a) Geometry of 2D pipe arrangement (b) 3D visualization with the simplify to be half in simulation

At high Reynolds numbers, the standard k-epsilon model avoids integrating the model equation through the wall by exploiting the near-wall behavior [14]. If y is the normal coordinate on the solid wall, the average velocity $30 < y_p^+ < 500$ satisfies the *log-*

law. Measurement of turbulent kinetic energy shows that the level of turbulence is the same as the rate of dissipation.

Geometry Model

The geometry is made according to the actual conditions, namely the critical area of the heat exchanger, a compact shell, and a tube heat exchanger.
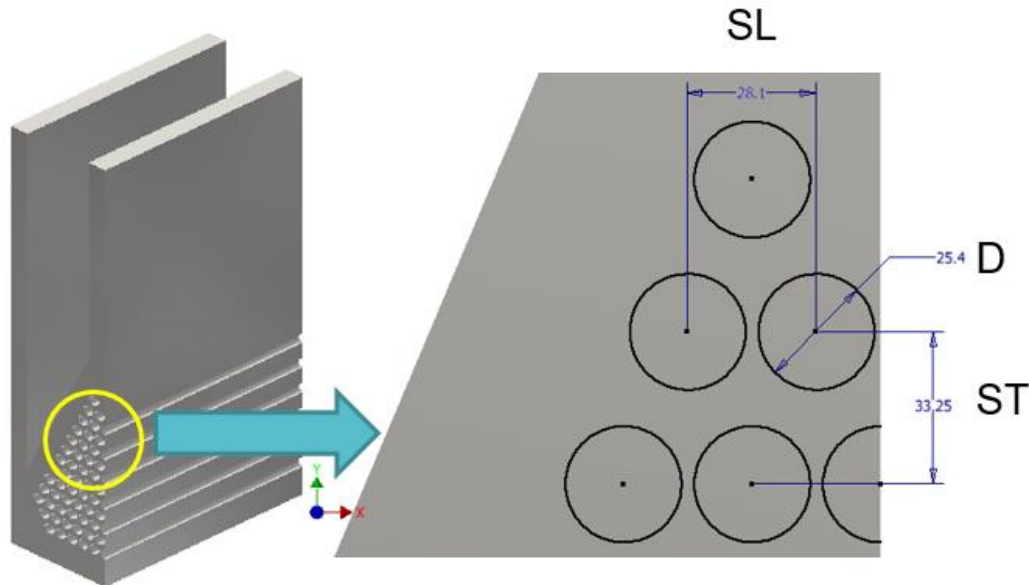

Figure 3. Detail tube arrangement in Geometry model

After the modelling process, the next step is to determine the boundary conditions in the model. The boundary condition used is the inlet, which is defined as the velocity of the inlet with the flow velocity assumed to be constant throughout the iteration and uniform throughout the inlet. Output (outlet) is defined as an outflow. This boundary condition is used because the flow parameters at the output are completely unknown. This boundary condition can only be used for incompressible fluids with the fully developed flow. The right and left shell walls are defined as walls. The pipe wall is defined as a wall. For pipes that are expected to know the value of the drag coefficient and heat transfer rate or Nusselt number, they are named pipe 1, pipe 2, pipe 3, and so on as desired. The area outside the pipe is defined as a vapor with a water vapor fluid material.

Table 1. Dimensions from geometry *tube banks*

Geometry	Unit
Diameter *tube* (D)	25.4 mm
Longitudinal distance (S_L)	28.1 mm
Transversal distance (S_T)	33.25 mm
Transverse pitch (P_T)	1.31
Longitudinal pitch (P_L)	1.11
Distance between pipe (vertical)	7.85 mm

Materials

The type of fluid material is water vapor (H_2O), and the type of solid material is Titanium (Ti) for the entire computational domain assuming constant properties as follows:

Table 3. Properties water vapor and titanium

Parameter	Properties	Value
Water vapor (H$_2$O)	*Density (kg m^{-3})*	0.5542
	Specific heat (J kg^{-1} K^{-1})	2014
	Absolute viscosity (kg m^{-1} s^{-1})	1,346x10^{-5}
	Thermal conductivity (W m^{-1} K^{-1})	0,0261
Titanium	*Density (kg m^{-3})*	4850
	Specific heat (kJ kg^{-1} K^{-1})	544.25
	Thermal conductivity (W m^{-1} K^{-1})	7.44
	Electrical conductivity (1/ohm.m)	2.381.000

Boundary Conditions

Determination of boundary conditions is one of the important steps of the solver. Errors in the assumption of boundary conditions will cause the simulation results to differ significantly from the experimental results. The inlet is defined as the inlet velocity with 37 m/s, while the temperature is 312K. The pipe is defined as a wall with a momentum value like the default Fluent, and the temperature is 305K. The area outside the pipe is defined as steam with water vapor material.

Table 4. Parameter variation geometry plate

Boundary condition	Parameter
Inlet	Type = *Velocity inlet*
	V$_{in}$ = 37 m s^{-1}
	T$_{in}$ = 312 K
Outlet	*Outflow*
Tube in the critical area	*Stationary wall*
	T$_w$ = 305 K
	Material titanium
Tube in other critical areas	*Porous media*
	T=305 K

Porous Media

Source term porous media consist of two components, namely viscous resistance, which is the inverse or opposite of permeability, namely the ability of the fluid to penetrate a porous media (α), and *inertial resistance* (C$_2$), which is the resistance of the flow of a fluid. The C$_2$ value can be calculated using the Van Winkle Equations, where for (thickness/diameter) > 1.6, and Reynolds Number >4000, the average C coefficient is 0.98, so the C$_2$ value can be calculated as:

$$C_2 = \frac{1}{C^2} \frac{(Ap/Af)^2 - 1}{t} \tag{1}$$

Where Af is Free area or total area, Ap is the area of plate (solid), C is A coefficient that has been tabulated for various Reynolds number range, and C$_2$ is Inertia resistance.

The results of C$_2$ are tabulated in table 5. *Viscous resistance* is an empirical value obtained from experimental results. However, if there are no experimental results, the value of viscous resistance is obtained by doing trial and error on Fluent and comparing the target pressure drop of the tube element with the total pressure drop of all tubes in the condenser tube arrangement.

Table 5. Element value porous media

Element type	C	*Thickness*	C_2
Porous_media	0.98	1	0.76

Meshing

The field or volume filled by the fluid is divided into small cells (meshing) so that the boundary conditions and some required parameters can be applied to the small elements. A pave and hexahedral cooper mesh is built in this research.
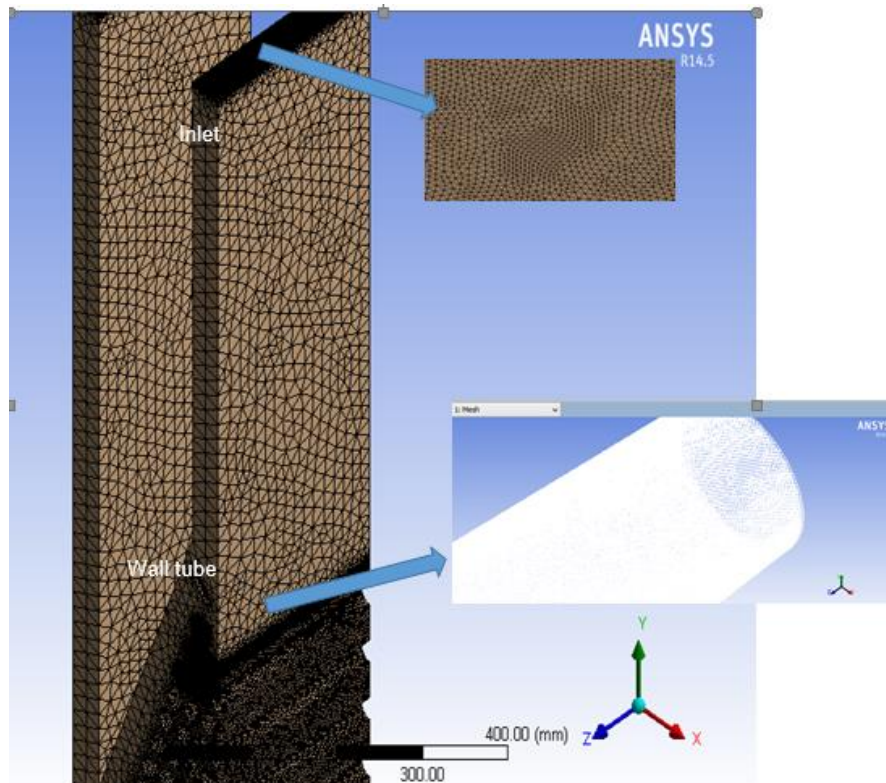

Figure 4. Detail Mesh in Geometry model

RESULTS AND DISCUSSION

This chapter presents qualitative and quantitative data on the effect of adding a device in the form of a plate to a staggered array of pipes in the critical area. Phenomenon and flow visualization are displayed in 3D from numerical simulations with CFD software ANSYS 14.5 mode focused on the critical area to explain the decrease in drag force that occurs in the critical area. Quantitative data in the form of pressure Coefficient (Cp). While the qualitative data is in the form of flow visualization (streamline velocity contour and pressure contour). Quantitative data in the form of pressure coefficients are displayed to predict changes that occur along the contour of the cylinder surface with the data collection point at the midspan

Position and Visualization model

Post-processing simulation results are carried out by looking at the distribution of pressure and Nusselt number on each tube in the critical area, speed, and temperature for each variation of the plate modification on the tube in the critical area. The simulation results data collection is done by performing iso-surface on XY are constantly shown in

Figure 5. Isosurface or midspan is to make an average data quantitative to get the best result in simulation. Visualization of the pressure contour is displayed isosurface by cutting XY coordinates. Other quantitative data in the form of speed and intensity of turbulence are obtained from the report – surface – integral – turbulent – turbulent intensity.
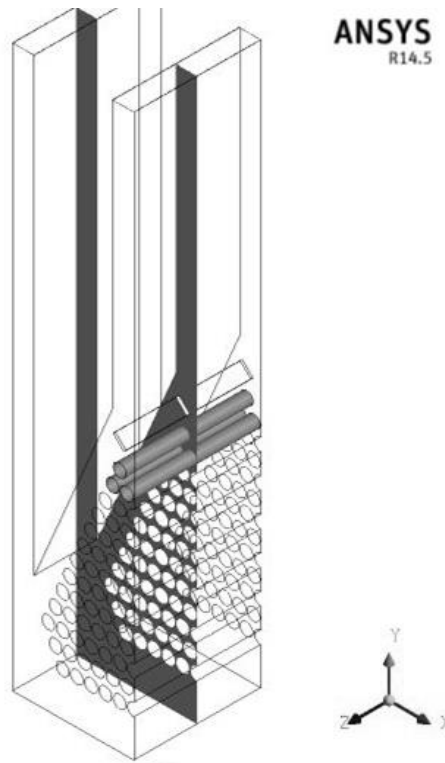
(a)

Figure 5. *iso-surface* XY *plane.*

The pressure coefficient is getting by numbering the tube. The tube number is the same as the inlet position shown in Figure 6.
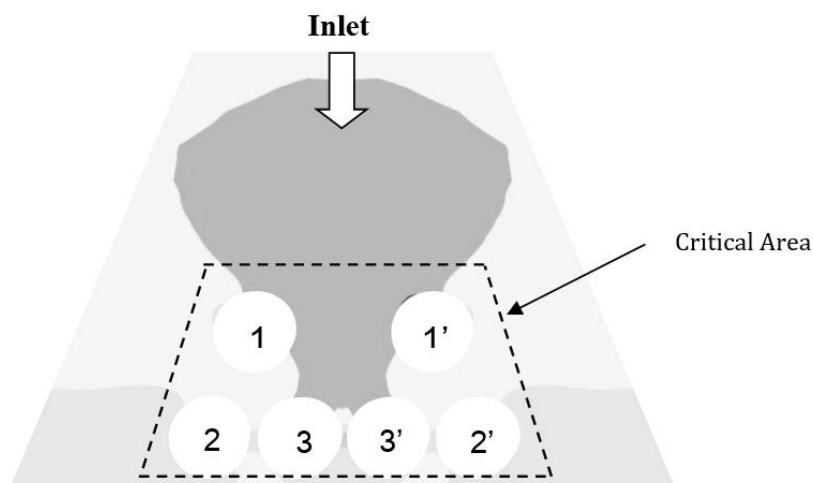

Figure 6. Numbering *tube* from the inlet

Grid independency

The structure of writing in this chapter begins with checking the grid (grid independence test) on several meshes that have been created. Furthermore, it is explained about the characteristics of flow and heat transfer in the tube numbering in the baseline configuration compared to the configuration of the addition of plate with three variation angles. Then a comparative analysis of numerical results with related references is carried out. This activity is a term used to describe simulation results in Fluent software that are not affected by mesh or grid size. This test needs to be done to ensure the accuracy and validity of the data from the numerical results.

Table 6. Grid independency

Mesh	Jumlah *Cell*	C_P	Validasi C_P [8]
A	1190636	-1.75	
B	1442276	-1.55	-0.5
C	1549558	-1	
D	**1815804**	**-0.476**	

The results of table 6 show that varying the number of cells near the wall, in the form of a y^+ approach, can increase the accuracy of the calculation. Furthermore, referring to mesh D, a study of the validity of the numerical method was developed by comparing the Cp from numerical results. Therefore, mesh D can be categorized as reasonable and feasible to be used as a reference in determining the grid number in the case of tube banks with guide plates.

Visualization of Pressure Coefficient Distribution to Predict Flow Characteristic

In this section, flow visualization in the form of pressure contours will be displayed to explain the pressure coefficient that occurs in the staggered pipe arrangement in the critical area. Qualitative data in the form of pressure contours in this critical area are shown in Figure 7 (a), namely the actual condition (baseline) and (b)(c) and (d) with the addition of plates at the angles of 15°, 30°, 45°. The pressure contour shown in Figure 4 is only for pipes in critical areas, namely 1st pipes, 2nd pipes, 3rd pipes, 4th pipes, 5th pipes, and 6th pipes. The contour in actual conditions or without flow disturbance plates shows high pressure on 1st pipes and 3rd pipes between 1600-1800 Pa at the top surface of the pipe.

The Figure above showed that this causes 1st and 3rd pipes to enter the critical area so that within a certain period, the pipes will quickly leak due to high pressure from the outside of the pipe. The high pressure in actual conditions is seen evenly in the area where the flow begins to hit the critical pipes. In a situation where the rectangular plate with the variation of 15 degrees to the y-axis is added, the most significant pressure occurs at the end of the disturbance plate, which is about 2000 Pa. The most significant pressure also still occurs on the surface of pipes 1 and 3. However, the pressure that occurs on pipes 1 and 3 has a smaller area when compared to the actual situation. Considerable pressures still occur in pipes 1 and 3 because the flow that goes to the critical pipe row hits the disturbance plate first and causes flow separation so that a wake is formed behind the plate. With the addition of a disturbance plate, the area of high pressure in the critical pipe area is reduced, and with the addition of a disturbance plate, the flow that previously would go directly to pipes 1 and 3 first hits the disturbance plate.
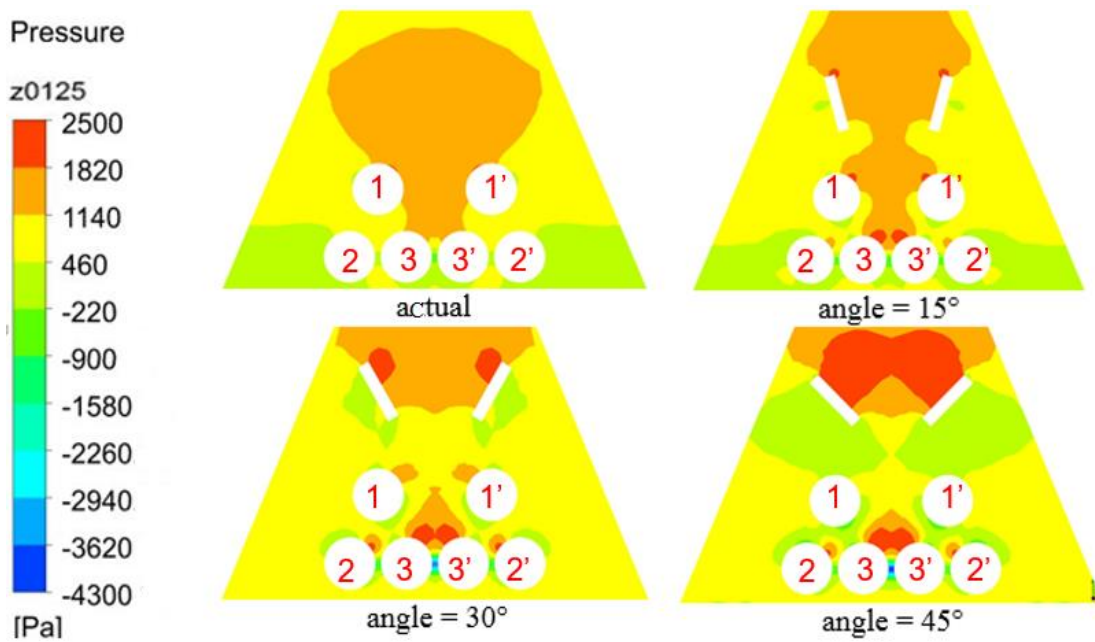
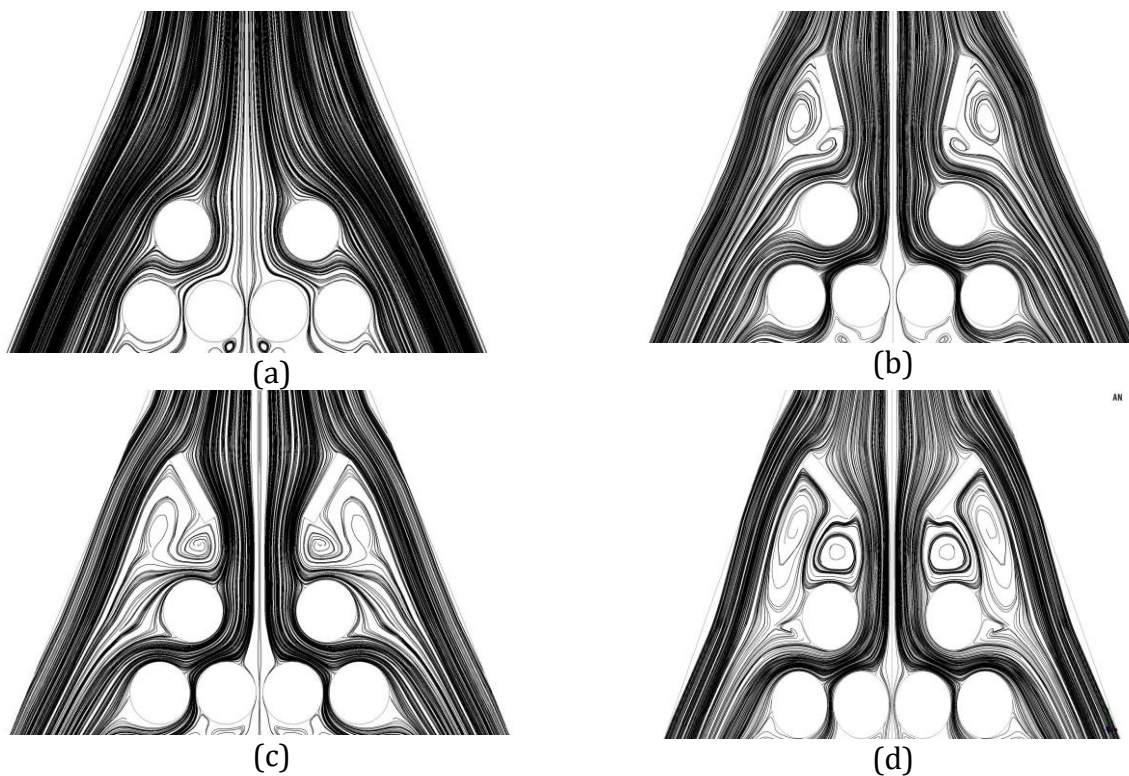**Figure 7.** Pressure contours under actual conditions and with modification angle

Figure 8. Velocity streamline in (a) actual conditions and with modification angle (b)15º, (c) 30º, and (d) 45º

The hypothesis of the addition of plates on the upstream side in the critical area aims to reduce pressure due to flow momentum, which has the potential to cause damage to pipes 1, 2, and 3. Moreover, save pipelines in critical areas. In row 2, there are tubes 2 and 3. In this position, when viewed from the XZ plane, it can be seen that the pressure contours that occur in both tubes are visible. It can be seen that when the pressure plate

is not disturbed, the pressure on tube 2 is around 500 Pa, and on tube 3 is 1400 Pa. On the visualization, by adding a nuisance plate on top of tube 1 with an angle of 15 degrees, it can be seen that on tubes 2 and 3, there is an increase in pressure. This is due to the flow separation that occurs on the interfering plate, so that it has an impact on the flow behind the plate. The flow behind the plate causes a vortex which increases pressure behind the flow separation so that the pressure on pipes 2 and 3 increases, namely on pipes 2 to 1100 Pa and in pipes 3 to 1800 Pa. The simulation results show that with the significant variation in the angle of the disturbance plate used to the y axis, the pressure that occurs in pipes 2 and 3 has increased to a pressure of 2300 Pa, and in conclusion, tube 1 and tube 2 are safe while tube 3 is damaged.

Figure 8 (a) shows a streamline at the XY plane position intersecting the z=0.125 axis in the critical region. Streamwise vortices interact with the boundary layer expressed in two dimensions and produce a swirling flow in which the flow occurs in the gap between row 2 and row 3. Then, (b) shows a streamline at the XY position on the variation plate addition with an angle of 15 degrees. The figure proves that the installation of the plate can produce streamwise vortices, which can cause fluid mixing, which is correlated with heat transfer. Continue in (c) if the modification plate is 30 degrees. Streamwise vortices interact with the boundary layer expressed in two dimensions and produce a mixed swirling flow between near wall and freestream flow. In general, mixing this flow can reduce the flow in the boundary layer, increase turbulence intensity, and create secondary flows that cause increased heat transfer. The vertical section clearly illustrates that adding the guide plate creates stronger eddies than the angle 15 degrees. The intensity of the eddies and number of vortices is higher than the other variations occurring at the variation angle of 30 degrees. The results in better heat transfer performance. At (d), streamwise vortices produce counter-rotating vortices which are displayed after hitting the plate. It should be noted that these vortices rotate upward of tube 1 in the critical region.
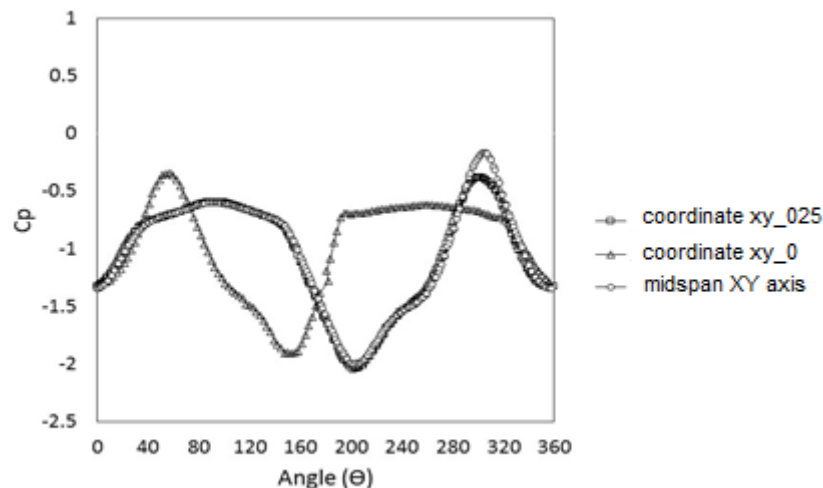

Figure 9. Graph *Cp* to *angle* with XY *plane* in angle 45 degrees

The graph of the pressure coefficient against the angle with the addition of a plate at an angle of 45 degrees is presented in Figure 9. The inlet_tube, midspan, and outlet_tube planes are made by cutting the Z-axis of the body. The trend of the inlet and outlet tube Cp values is the same, while the midspan is slightly shifted to the left and the increase is more stable. Furthermore, data collection and contours are used in the midspan area to maintain data uniformity. The distribution of the pressure coefficient for the midspan

position in the baseline condition compared to the condition with the addition of modification variations in the angle on the plate is shown in figure 9. The pressure coefficient distribution, which is similar to various variations and disturbances with variations in angle, has been described by Alam et al. [15], partly done by Qiu [7] to make sure distribution pressure coefficient into one graph as validation.
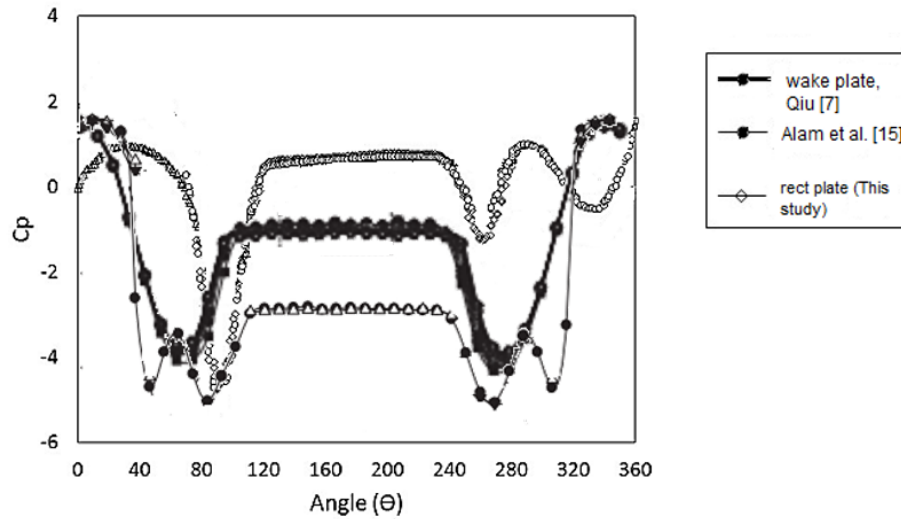

Figure 10. The mean pressure distribution for a cylinder with a modification plate based on Alam [15] and Qiu [7]
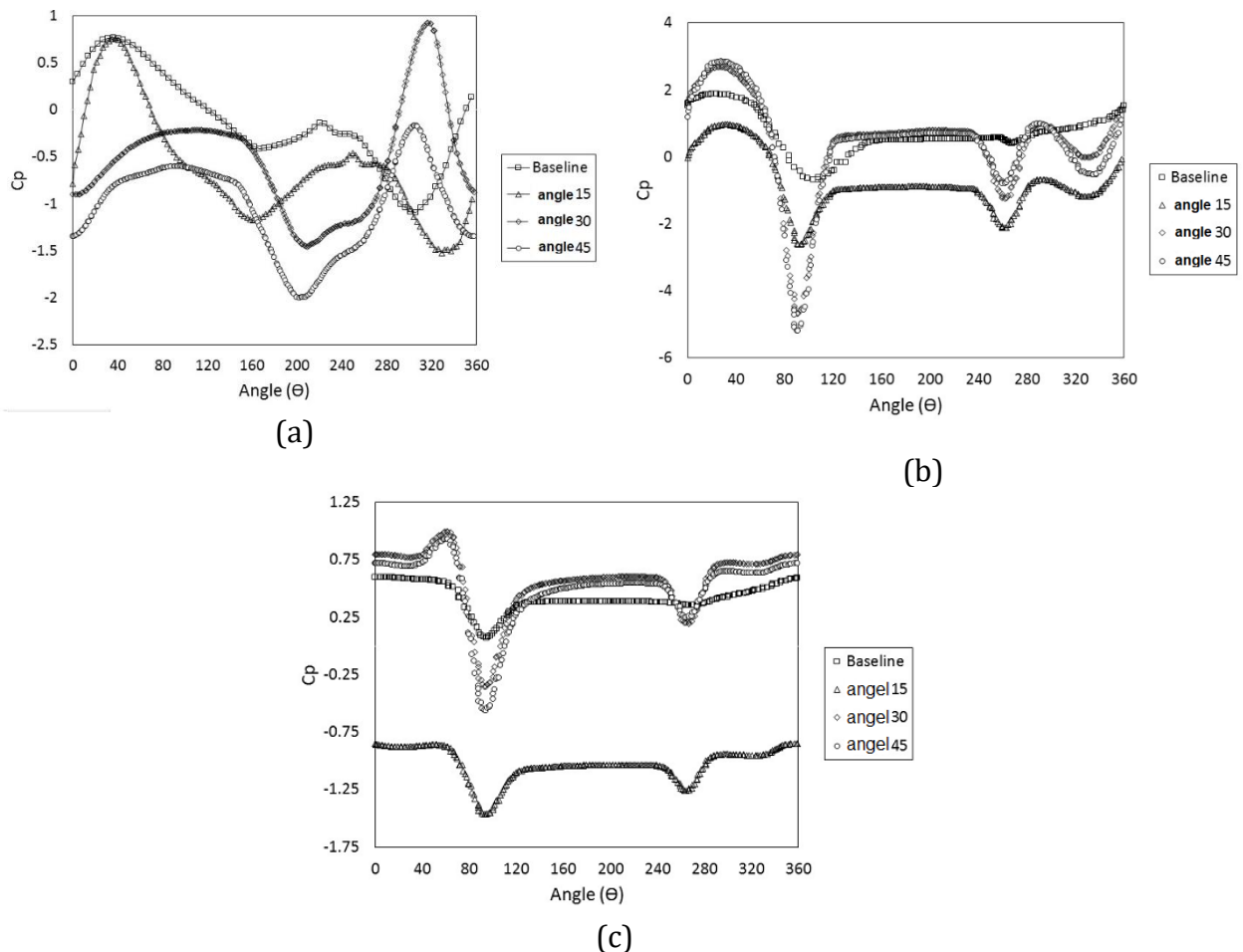

(a)

(b)

(c)

Figure 11. Pressure Coefficient baseline and modification angle at (a) 1st tube (b) 2nd tube (c) 3rd tube

The pressure coefficient distribution is only observed in the critical tube (tube 1), which is indicated to have the most significant pressure due to the dynamic force that hits the tube. The graph shows that the stagnation point is not precisely at position 0 degrees because the maximum Cp value in that figure is not at position 0 degrees.

Figure 11. (a) The position where Cp is maximum and the fluid velocity is zero is called the stagnation point. Stagnation where the fluid flow at high speed must stop before hitting the tube to reach its maximum pressure. From this picture, the stagnation point at the baseline position is at position 45 degrees (x-axis). It can be seen that the stagnation point is not precisely at position 0 but shifted. The shift of the stagnation point is influenced by the direction of the fluid flow that leads to the left, following the shape of the tube arrangement that resembles a diffuser before hitting the critical tube. From the Figure 11. (b) after the stagnation point, the flow accelerates, which is indicated by a decrease in the graph of the pressure coefficient. The flow has a maximum speed which is indicated by the lowest pressure coefficient distribution value. On the upper side, the flow experiences a maximum velocity at an angle of about 40-90 degrees, while on the lower side, the flow experiences a maximum velocity at an angle of 240- 260 degrees. Then the flow slows down due to adverse pressure, which is marked by an increase in pressure. At one point, the flow can no longer resist the adverse pressure and friction, so separation occurs, which is indicated by the pressure coefficient value starting to steady at an angle of 120 degrees for the upper side and 240 degrees for the lower side in all conditions. Figure 11. (c) shows the pressure coefficient distribution that occurs in tube 3. After the stagnation point, an acceleration is indicated by the Cp value gradually decreasing until there is a maximum acceleration at an angle of 70-90 degrees for the baseline condition on the upper side and the angle 240-280 degrees on the lower side. Due to the adverse pressure gradient, the flow slows down at an angle of 90-130 degrees on the upper side and 290- 320 degrees on the lower side.

CONCLUSIONS

The simulation results show that based on the pressure contour in the baseline pipe arrangement, there is high pressure in the critical pipe so that the area is called the critical area. Modifying the pipe arrangement by installing the plate before the flow hits the pipe arrangement in the critical area with plate angle (α= 15°, 30°, and 45°) is carried out to reduce the drag force on the critical area by maintaining optimal heat transfer. The result is the total drag coefficient (C_d), representing the FD in the modified pipe arrangement with the addition of the average plate being reduced compared to the average Cd in the baseline pipe arrangement. Sequential C_D values from baseline conditions and angle variation (α= 15°, 30°, and 45°) are 0.537; 0.644; 0.446; 0.464. Considering the above aspects, in this study, the most optimal plate is the angle of (α=30°). The simulation results show that changing the plate angle variation can reduce the Nusselt value compared to the baseline condition.

DECLARATION OF CONFLICTING INTERESTS

The author(s) declared no potential conflicts of interest with respect to the research, authorship, and/or publication of this article.

FUNDING

REFERENCE

[1]   M. M. El-Wakil, Powerplant Technology, McGraw-Hill Book Co, 1985

[2]   Haldkar Vikram (Dec 2013) "Parametric analysis of surface condenser for thermal power plant," Gyan Ganga Institute of Engineering and Technology Jabalpur M P India.

[3]   P. Mirzabeygi and C. Zhang, "Three-dimensional numerical model for the two-phase flow and heat transfer in condensers," International Journal of Heat and Mass Transfer, vol. 81, 2014.618-637

[4]   Zeng, H., Meng, J. A., and Li, Z., 2012, "Numerical Study of a Power Plant Condenser Tube Arrangement," Appl. Therm. Eng., 40, pp. 294–303.

[5]   NUS Training Corporation, Power Principle, Power Plant Series: Turbine, 1981.

[6]   Hitachi Machinery & Engineering, LTD, Instruction Manual of Steam Surface Condenser and Accessories, 1997.

[7]   Qiu, Y., Sun, Y., Wu, Y., Tamura, Y., (2014). "Effects of Splitter Plates and Reynolds Number on the Aerodynamic Loads Acting on Circular Cylinder", Jurnal Wind Engineering, Vol. 127, pp. 40-50

[8]   Chakrabarty S.G, (2012), "Flow and Heat Transfer Behaviour Accros Circular Cylinder and Tube Bank With and Without Splitter Plate", Nagpur India

[9]   Hui Zeng, Ji'an Meng, Zhixin Li (2012). "Numerical study of a power plant condenser tube arrangement", Applied Thermal Engineering, Vol. 40, pp. 294-303.

[10] Vedran Medica-Viola, Branimir Pavkovic, Vedran Mrzljak (2018). "Numerical Model for on-condition monitoring of condenser in coal-fired power plants", International Journal of Heat and Mass Transfer, Vol. 117, pp. 912-923.

[11] P. Chu, Y.L. He, Y.G. Lei, L.T. Tian, R. Li, (2009), "Three-dimensional numerical study on fin and oval-tube heat exchanger with longitudinal vortex generators", Appl. Therm. Eng., Vol. 29, pp. 859–876.

[12] Babak Lotfi, Min Zeng, Bengt Sund, Qiuwang Wang, (2014), "3D numerical investigation of flow and heat transfer characteristics in smooth wavy fin-and-elliptical tube heat exchangers using new type vortex generators", Journal of Energy, Vol. 73, pp. 233-2576.

[13] Zhang, C., 1994, "Numerical Modeling Using a Quasi-Three-Dimensional Procedure for Large Power Plant Condensers," ASME J. Heat Transfer, 116(1), pp. 180–188

[14] H K Versteeg and W Malalasekera, (2007), An Introduction to Computational Fluid Dynamics The Finite Volume Method, 2nd edition, Pearson Prentice Hall, U.K.

[15] Alam, M.D., Sakamoto. H., Moriya, M., (2003). "Reduction of fluid forces acting on a single circular cylinder and two circular cylinders by using tripping rods". Journal of fluids and structures, Vol. 18, 347-366.